JLB | JOURNAL OF LEUKOCYTE BIOLOGY

ARTICLE

Inducing regulated necrosis and shifting macrophage polarization with anti-EMMPRIN antibody (161-pAb) and complement factors

Nizar Hijaze[1] | Max Ledersnaider[2] | Elina Simanovich[2] | Sameer Kassem[1,3] | Michal A. Rahat[2,3] (iD)

[1]Department of Internal Medicine A, Carmel Medical Center, Haifa, Israel

[2]Immunotherapy Laboratory, Carmel Medical Center, Haifa, Israel

[3]Ruth and Bruce Rappaport Faculty of Medicine, Technion-Israel Institute of Technology, Haifa, Israel

Correspondence
Michal A. Rahat, Immunotherapy Laboratory, Carmel Medical Center, 7 Michal St., Haifa, 34362112, Israel
Email mrahat@netvision.net.il

Abstract

Treatment of solid tumors is often hindered by an immunosuppressive tumor microenvironment (TME) that prevents effector immune cells from eradicating tumor cells and promotes tumor progression, angiogenesis, and metastasis. Therefore, targeting components of the TME to restore the ability of immune cells to drive anti-tumoral responses has become an important goal. One option is to induce an immunogenic cell death (ICD) of tumor cells that would trigger an adaptive anti-tumoral immune response. Here we show that incubating mouse renal cell carcinoma (RENCA) and colon carcinoma cell lines with an anti-extracellular matrix metalloproteinase inducer polyclonal antibody (161-pAb) together with complement factors can induce cell death that inhibits caspase-8 activity and enhances the phosphorylation of receptor-interacting protein kinase 3 (RIPK3) and mixed-lineage kinase-like domain (MLKL). This regulated necrotic death releases high levels of dsRNA molecules to the conditioned medium (CM) relative to the necrotic death of tumor cells induced by H_2O_2 or the apoptotic death induced by etoposide. RAW 264.7 macrophages incubated with the CM derived from these dying cells markedly enhanced the secretion of IFNβ, and enhanced their cytotoxicity. Furthermore, degradation of the dsRNA in the CM abolished the ability of RAW 264.7 macrophages to secrete IFNβ, IFNγ-induced protein 10 (IP-10), and TRAIL. When mice bearing RENCA tumors were immunized with the 161-pAb, their lysates displayed elevated levels of phosphorylated RIPK3 and MLKL, as well as increased concentrations of dsRNA, IFNβ, IP-10, and TRAIL. This shows that an antigen-targeted therapy using an antibody and complement factors that triggers ICD can shift the mode of macrophage activation by triggering regulated necrotic death of tumor cells.

KEYWORDS
dsRNA, EMMPRIN/CD147, IFN response, macrophage polarization, regulated necrosis, tumor microenvironment

1 | INTRODUCTION

The tumor microenvironment (TME) is critical for tumor angiogenesis, progression, invasion, and metastasis. The biochemical characteristics of the TME (i.e., hypoxia, acidosis, increased extracellular matrix stiffness) drive tumor cells to adapt their metabolism, enhance angiogenesis, and activate transcriptional programs that promote tumor growth and metastasis.[1] They also influence different types of stroma cells, particularly tumor-associated macrophages (TAMs), that interact with the tumor cells to produce myriad enzymes, cytokines, chemokines, and growth factors (e.g., matrix metalloproteinases-MMPs, VEGF, HGF, CXC12/SDF-1, TGFβ, IL-10) that collectively support tumory growth and suppress effector immune cells that could attack tumor

---

cells.[2] This dynamic TME is also involved in the development of cancer resistance to therapy, including chemotherapy, radiotherapy and targeted therapy, resistance that arises from both the tumor cells (e.g., increased mutation rate, epigenetic changes, inhibition of apoptosis), and stroma cells. Mechanisms that mediate such resistance in the stroma cells are under investigation, and they may include inability to recruit effector T cells to the tumor site, or to prime them.[3] Moreover, hypoxia and acidity may be increased during chemotherapy or radiotherapy,[2] thus preventing efficient drug distribution.[4] Therefore, targeting the TME to normalize vasculature and enhance immune response against the tumor has become an important goal.[5]

Immunogenic cell death (ICD) of tumor cells is induced by antitumoral agents and results in the activation of an adaptive antitumoral response against antigens of the dying cell.[6] ICD can be triggered by different cell death mechanisms, including autophagy, necrosis, or regulated necrosis, as opposed to caspase-dependent apoptosis that is considered nonimmunogenic. Specifically, necroptosis is a form of regulated necrosis that can be triggered by ligation of several death receptors (e.g., TNFR, FAS, TRAILR1/DR4).[7] This ligation activates the receptor-interacting protein kinase 1 (RIPK1) and RIPK3, and if ubiquitination of RIPK1 is low and caspase-8 activity is inhibited, promotes the assembly of the necrosome that consists of activated RIPK1, RIPK3, and the mixed-lineage kinase domain-like protein (MLKL) to induce ICD by necroptosis. Radiotherapy and some chemotherapies (e.g., anthracyclines, cyclophosphamide, doxorubicin, but not etoposide[8,9]) successfully induce ICD as part of their mechanism of action.

ICD initiates a cascade of events, starting from the release of specific danger-associated molecular patterns (DAMPs) that act as adjuvants and recruit dendritic cells to the tumor site. Only few DAMPs have been directly linked to ICD,[6] and these include extracellular ATP,[10] secreted high mobility group box 1,[11] membranal expression of calreticulin,[12] cancer-derived nucleic acids,[13] including dsRNA,[14] annexin-1,[15] and type I IFNs.[16] When released, these DAMPs bind to their respective pattern recognition receptors on innate immune cells and activate them. Necroptosis, in particular, has been shown to trigger innate and adaptive immunity,[7,17,18] potentially leading to alleviation of the immunosuppressive TME.

Extracellular matrix metalloproteinase inducer (EMMPRIN)/CD147 is a multifunctional protein, which is overexpressed in many types of tumor cells, can interact with many proteins to regulate tumor cells metabolism, angiogenesis, proliferation, and metastasis, and therefore represents a promising anti-cancer target.[19,20] We have recently targeted a specific epitope on EMMPRIN in tumor-bearing mice with an antibody[21] or with an octa-branched, multiple antigenic peptide (MAP) that was synthesized with this epitope sequence (designated 161-MAP).[22] Both methods significantly inhibited tumor growth and metastasis in several mouse models. This was attributed to the marked reduction in angiogenesis and proliferation of tumor cells. Most importantly, both active and passive vaccinations alleviated the immune suppression that characterizes the TME, as observed by the reduction in TGFβ levels, and increased infiltration of macrophages and CD8^{+} T cells, as well as their enhanced

cytotoxicity, demonstrating the activation of the adaptive immune system. However, the mechanism that allowed such a shift in the TME remained unclear.

Here we demonstrate that the antibody targeting EMMPRIN in the presence of complement factors cause death of tumor cells by regulated necrosis, leading to the release of the potent DAMP dsRNA and a shift in macrophage polarization.

2 | METHODS

2.1 | Cells and experimental procedure

The tumorigenic mouse renal (RENCA, ATCC CRL-2947) and colon (CT26, ATCC CRL-2638) carcinoma cell lines were cultured in RPMI-1640 medium, 10% FCS, 1% l-glutamine, and antibiotics. HEPES buffer (100 mM, pH 7.4) was added to the RENCA medium, and 1% sodium pyruvate was added to the CT26 medium. The macrophage-like RAW 264.7 cell line (ATCC TIB-71), was cultured in DMEM with 10% FCS, 1% L-glutamine, and antibiotics. Cells were split every 3–4 d at a ratio of 1:4 using trypsin-EDTA. All cell lines were routinely checked for morphologic changes and presence of mycoplasma and were used at passages 3–15.

Cells were seeded in 24-well plates (2–4 $\times$ 10^5 cells/500 μl) or 96-well plates (0.5–5 $\times$ 10^4 cells/100 μl) in serum-starvation medium to avoid potential masking of signals. Tumor cells were incubated without any inducer as controls, or were induced to die by necrosis using H$_2$O$_2$ (100 μM, 323381, Sigma-Aldrich Corp. St. Louis, MO, USA) or by apoptosis using Etoposide (10 μM, ab120227, Abcam, Cambridge, United Kingdom). Alternatively, tumor cell death was induced by addition of 161-pAb (0.64 μg/ml, produced in our lab by vaccinating rabbits as described before[21]) together with 1:50 (v/v) complement proteins (C201-0005, Rockland Antibodies & Assays Limerick, PA, USA). The concentrations of the cell death inducers were first calibrated (Supporting Information Fig. S2). In some experiments, conditioned media derived from the cells induced to die with 161-pAb and complement was digested with RNAse III (10 U/ml for 30 min at 37°C, New England Biolabs, Ipswich, MA, USA).

2.2 | Sandwich ELISA

The mouse TNFα, IL-1β, IL-10, TGFβ, IFNβ, IFNγ-induced protein 10 (IP-10), and TRAIL concentrations were determined using DuoSet ELISA kits (R&D Systems, Minneapolis, MN) according to the manufacturer's instructions. Complement activation was determined using the mouse ELISA kit for C3a (TECO medical AG, Sissach, Switzerland), and the Granzyme B uncoated ELISA kit (Thermo Fisher Scientific, Waltham, MA, USA) was used to evaluate the amounts of the enzyme.

In-house dsRNA sandwich ELISA was carried out as described before.[23,24] Plates were coated with 0.4 μg/well protein A (P7837, Sigma) overnight at 4°C. The plates were then incubated with blocking buffer (0.1 M NaH$_2$PO$_4$, 0.1 M Na$_2$HPO$_4$, pH 6.8, 0.025% merthiolate, 0.5% BSA, and 0.05% Tween 20) for 1 h at 37°C and then with 1 μg/ml of the monoclonal anti-dsRNA J2 antibody (SCICONS, English

Scientific Consulting, Szirak, Hungary) overnight at 4°C. Wells were washed three times (0.5% Tween 20 in PBS) and supernatant samples were then added at a dilution of 1:100 in blocking buffer for 2 h. After three washes, the monoclonal anti-dsRNA K2 antibody (SCICONS, English Scientific Consulting) diluted 1:10 was added for additional 2 h. Both J2 and K2 monoclonal antibodies are known to recognize dsRNA helixes greater than 40 bp, including the synthetic poly (I:C).[24] After three washes the plates were incubated with biotinylated goat anti-mouse IgM (115-066-075, Jackson Immuno-Research Labs, West Grove, PA, USA) diluted 1:1000 in blocking buffer for 1 h at room temperature, washed again three times, and incubated with streptavidin-HRP diluted 1:200 in block buffer. Finally, TMB was added for 5 min and absorbance was read at 450 nm with reference at 540 nm. Final concentrations were calculated according to a standard curve of known concentrations of poly (I:C).

2.3 | Western blot analysis

Equal amounts of the tumor cell lysates (15 μg/lane) were denatured and loaded unto 12% SDS-polyacrylamide gel, and separated by electrophoresis for 2 h at constant voltage of 150 V. Proteins were transferred onto nitrocellulose membranes (L-08003-010, Advansta, San Jose, CA, USA), and the membranes were blocked with AdvanBlock-Chemi (R-03726-E10, Advansta) overnight at 4°C. Then membranes were incubated with the primary antibodies (rabbit anti-human MLKL, rabbit anti-human phosphorylated-MLKL, rabbit anti-human RIPK3, mouse anti-human phosphorylated-RIPK3, or the mouse anti-β-actin, all from Abcam) diluted 1:1000 in the blocking buffer for 1 h at room temperature. Membranes were washed three times (1× TBS with 0.05% Tween-20) and incubated with HRP-conjugated secondary antibody (goat anti-mouse IgG or donkey anti-rabbit IgG, Jackson Immuno-Research Labs) diluted 1:5000 in blocking buffer. After three additional washes, membranes were incubated with Western Bright ECL-HRP substrate (K-12045, Advansta), and protein bands were visualized using the Omega Lum G Imaging System (Aplegen, Pleasanton, CA, USA). Membranes were then stripped and reprobed with anti-β-actin to demonstrate equal loading. Protein bands were quantified using the ImageJ software.[25]

2.4 | Immunofluorescence

RENCA or CT26 cells (250,000 cells/well) were seeded on sterile cover slips and subjected to the experimental procedure and then fixed with cold methanol for 5 min. Cells were permeabilized with 0.25% Triton X-100 in PBS for 10 min and incubated in blocking solution (4% normal goat serum, 4% normal donkey serum, 0.1% Triton X-100 in PBS) for 30 min at room temperature. Then cells were incubated overnight at 4°C with the primary antibodies (mouse anti-human phospho-RIPK3, ab205421, and rabbit anti-human phosphorylated-MLKL, ab187091, both from Abcam) diluted 1:250 in blocking solution. After three washes, cells were incubated with secondary antibodies (PE-conjugated goat anti-mouse IgG, 115-116-146, Jackson Immuno-Research Labs, and Alexa Fluor 488-conjugated donkey anti-rabbit

IgG, ab150061, Abcam) diluted 1:500 in 1× PBS for 2 h at room temperature. Coverslips were mounted on a slide with Fluoromount-G and images were acquired by upright fluorescent trinocular microscope (Olympus BX-60, Tokyo, Japan) using the MS60 camera and the MShot Image Analysis System V1 (MSHOT, Guangzhou Micro-shot Technology Co., Guangzhou, China).

2.5 | Caspase activity

The caspase-3 and caspase-8 activity assays (K106 and K113, Biovision, Milpitas, CA, USA) determine the enzymatic activity of each caspase by measuring the colorimetric signal emitted by the cleavage of a caspase-specific substrate (the peptide sequences DEVD and IEDT, respectively) labeled with the chromophore p-nitroanilide (pNA), using a microplate reader (DTX880 Multimode Detector, Beckman Coulter, Pasadena, CA, USA). A total of 5×10^5 tumor cells/well were seeded in a 24-well plate and subjected to the experimental procedure. Cell lysates were prepared according to kit protocol and the total protein concentrations of each lysate were determined using Bradford Ultra reagent (BFU05L, Expedeon, Cambridge, United Kingdom). A total of 50 μg protein and 100 μg protein per sample were used for the caspase 3 and caspase 8 activity assays, respectively. Absorbance was measured at 405 nm.

2.6 | Cell viability assay

Tumor cells were seeded (5×10^4 cells) in 96-well plates and subjected to the experimental conditions. After 24 h, 10 μl of the cell counting kit 8 (CCK-8, 96992, Sigma) reagent was added to 100 μl of serum-free medium. After 1 h at 37°C, the WST-8 (2-(2-methoxy-4-nitrophenyl)-3-(4-nitrophenyl)-5-(2,4-disulfophenyl)-2H-tetrazolium, monosodium salt), tetrazolium salt was taken up and reduced in the mitochondria of viable cells to a soluble orange formazan dye, and the absorbance that is directly proportional to the number of viable cells could be measured at 450 nm with 540 nm reference.

2.7 | Lactate dehydrogenase (LDH) activity assay

LDH activity in cell supernatants was measured by the rate of reduction of NAD$^+$ to NADH by LDH after addition of the LDH reaction mix according to the kit protocol (ab102526, Abcam). LDH activity was calculated according to the color produced at 450 nm at two time points, according to the kit instructions.

2.8 | ATP detection assay

The concentrations of extracellular ATP in the supernatants of cell cultures were measured using the Luminescent ATP Detection Assay Kit (ab113849, Abcam). Luciferase and its substrate luciferin were added to supernatant samples in a black 96-well plate, where presence of ATP resulted in photon emissions, which were detected by a microplate luminometer (DTX880 Multimode Detector, integration time 1000 ms), and compared to a standard curve with known ATP

concentrations. Endogenous ATPase activity was inhibited by the kit buffer.

2.9 | Cell cytotoxicity assay

Tumor cells were labelled with 2.5 μM Cell Tracker Orange CMTMR Dye (C2927, Thermo Fisher Scientific) according to reagent protocol, washed to remove excess dye, counted and seeded in a 96-well plate. The fluorescent dye freely enters the cells, where it is esterified to become impermeable. Tumor cells were incubated in media without phenol red, to avoid its fluorescence, and were induced to die according to the experimental procedure. The supernatants were transferred to a black 96-well plate to measure the fluorescent signal spilled to the medium. Percentage of dead cells was calculated using the equation:

$$\text{Cytotoxicity } (\%) = \frac{(\text{RFUsample} - \text{RFUspontaneous})}{(\text{RFUmaximum} - \text{RFUspontaneous})} \times 100$$

Detection of DNA fragmentation by ELISA to detect the release of histone-associated DNA fragments that are typical of apoptotic death, the Cell Death ELISA[plus] kit (11774425001, Sigma) was used. Tumor cell lysates were prepared according to manufacturer's instructions and total protein concentrations were determined using Bradford Ultra Reagent (Expedeon). A mixture of two antibodies was added to the cell lysates, where the biotinylated anti-histone antibody that recognizes histone proteins was captured onto the streptavidin-coated microplate, and the anti-DNA antibody that recognizes single or double-stranded DNA sequences was linked to HRP. After washing, the HRP substrate was added and the incubated for 20 min. Absorbance was measured at 405 nm with a reference of 490 nm according to kit specifications.

2.10 | TUNEL assay

The TUNEL assay was carried out according to the kit instructions (In Situ BrdU-Red DNA Fragmentation-TUNEL Kit, ab66110, Abcam). Briefly, 4×10^5 tumor cells were seeded on cover slips and subjected to the kit protocol. Then cells were fixed with 4% paraformaldehyde and permeabilized with 20 μg/ml proteinase K and DNA was labeled with Br-dUTP, washed and stained with the fluorescent anti-BrdU-Red that recognizes 3′-OH on nicked-ends of DNA, and with the fluorescent stain 7-AAD that binds to GC-rich regions of DNA in the cells. Labelled cells were visualized using the fluorescent microscope and images were captured at a magnification of ×250 from at least three different fields. The percentage of double-positive cells was quantified using ImagePro 4.5 software (Media Cybernetics, Inc., Rockville, MD, USA).

2.11 | In vivo mouse model

Vaccination of tumor-bearing mice with the 161-pAb was carried out as described before.[21] Briefly, 2×10^6 RENCA cells were mixed in 200 μl of matrigel, and were subcutaneously injected to the flank of BALB/c mice (female, 8 wk old) to generate tumors. By day 12, when tumors were already palpable, mice were i.p. injected with either an irrele-vant antibody (rabbit IgG) or with the 161-pAb (50 μg per 25 g body weight each) in three boost injections every 7 d. A total of 39 d after the implantation of the tumor cells, mice were euthanized and parts of the tumors were freshly frozen for later analysis by Western blot analysis and sandwich ELISA.

Mice were purchased from Harlan Laboratories (Jerusalem, Israel), and cared for in accordance with the procedures approved by the Supervision of Animal Experiments Committee at the Technion (Haifa, Israel; IL-1231013) and outlined in the NIH guideline for the care and use of laboratory animals.

2.12 | RNAseq data analysis

Our previous RNAseq data were deposited before (NCBI's Gene Expression Omnibus, GEO Series accession number GSE854400). For selected genes, previously grouped into the innate immunity and IFN response metagroups,[22] the normalized counts were calculated using DESeq2 and log base 2 transformed. For each gene the gene's mean (taken over all samples) was subtracted. The heat map was launched using scale = "none." This part of the study was conducted by the Genomic Center of the Biomedical Core Facility, at the Faculty of Medicine, Technion.

Quantitative real-time PCR (qPCR): The total RNA was extracted from mouse tumor tissues using the total RNA purification kit (Norgen Biotek, Horold, Ontario, Canada), and 2 μg from each sample were transcribed to cDNA using the qScript cDNA synthesis kit (Quantabio, Beverly, MA, USA). Expression of CD38, iNOS, CD206, and arginase-I mRNAs and their reference gene PBGD was determined using the PerfeCTa SYBR green Fastmix (Quantabio) with the StepOne system (Applied Biosystems, Foster City, CA, USA) in triplicates according to the manufacturer's instructions. The comparative CT method was used for relative quantification with one of the Rb-IgG immunized mice serving as the calibrator for all samples. Primers used are listed in Supporting Information Table S1.

2.13 | Immunohistochemistry

Antigen retrieval for C3d and CD8 were carried out by microwave heating in citrate buffer (pH 6.0). The 4-μm-thick paraffin sections were stained with either the goat polyclonal anti-C3d antibody (R&D Systems) in a 1:40 dilution or the rabbit polyclonal anti-CD8 antibody (Bios, Woburn, MA, USA) diluted 1:400. Sections were washed, and the antibodies were detected with the ZytoChem Plus HRP-Polymer anti-rabbit (Zytomed, Berlin, Germany) or with donkey anti-goat IgG diluted 1:500 (Jackson Immuno-Research Labs) for 1 h, then the DAB substrate was added (Zytomed) and finally the sections were counter-stained with hematoxylin (Sigma). All sections were viewed under the bright field trinocular microscope (Olympus BX-60) and images were acquired with the MS60 camera and the MShot Image Analysis System V1 (MSHOT, Guangzhou Micro-shot Technology Co.). The amount of C3d bound to the tumor cells was assessed using the ImagePro plus 4.5 software (Media Cybernetics, Inc.) and calculated using the H-score (as described in Simanovich et al.[26])

2.14 | Statistical analysis

All experiments were independently repeated at least four times and results are represented as mean ± SEM. Statistical significance between three groups or more was determined using one-way ANOVA with Bonferroni's post-hoc multiple comparison test, and between two groups using the Student's unpaired t-test. Statistical significance was achieved at P-values less than 0.05 ($\alpha < 0.05$).

3 | RESULTS

3.1 | Mice vaccinated with 161-MAP show increase in genes related to antiviral response

We used the previously reported RNAseq data derived from tumor-bearing mice vaccinated with 161-MAP and compared to control mice vaccinated with the scrambled peptide (Scr-MAP),[22] to further analyze the influence of the vaccination process on the expression of selected genes. Previously, these genes were grouped in two meta-groups belonging to IFN response and innate immunity. Upon further analysis of the RNAseq data, we observed a significant increase by more than 1.8-fold in 38 genes that are associated with an antiviral response and/or are induced by IFN (IFN-stimulated genes-ISG). These included (i) several sensors of nucleic acids, particularly of dsRNA (*ddx58/RIG-1*, *dhx58*, *fihi1/mda5*, *tlr3*, *tmem173/sting*, *zbp1/DAI*, *nod1*, *nod2*); (ii) activators of RNAse L and inhibitors of replication and protein synthesis (*oas2*, *oas3*, EIF2AK2/*pkr*, *Mx1* and *Mx2*); (iii) E3 ligases and deubiquitinases that are involved in the inhibition of the NF-κB pathway, induction of necroptosis, and in the regulation of the IFN pathway (*Cyld*, *Rnf125*, *Trim25*, *Ups18*, *Isg15*, *Trim30a*); (iv) the caspase inhibitor *Xiap*; and (v) transcription factors linked to the IFN pathway (*Irf7*, *Stat2*) (Supporting Information Fig. S1). Despite the variability between the 161-MAP vaccinated tumors, these genes were considerably elevated relative to the control tumors vaccinated with the scrambled peptide. Thus, we concluded that an anti-tumoral response that resembles an antiviral response with an ISG signature is initiated by the 161-MAP vaccination process, a response involving recognition of nucleic acids, particularly dsRNA, and triggering an IFN response. This conclusion was the conceptual basis for the current study.

3.2 | 161-pAb together with complement factors kill tumor cells

To explore whether the anti-EMMPRIN polyclonal antibody (161-pAb) kills tumor cells efficiently, we first calibrated the in vitro system. We used the mouse CT26 colon carcinoma and RENCA renal carcinoma cells, and incubated them with increasing amounts of the antibody in the presence of complement factors (Supporting Information Fig. S2A), and then with increasing dilutions of the complement reagent (Supporting Information Fig. S2B). Both cell types demonstrated reduced viability at a concentration of 0.64 μg/ml of the antibody, and a dilution of 1:50 of the complement factors was sufficient to drive cell death

with the antibody ($P < 0.01$), and thus we have used these concentrations in all following experiments. As expected, the antibody alone or the complement factors alone did not induce death, and only their combination resulted in decreased cell viability. To compare the efficiency of tumor cell death induced by the antibody and complement to other death-inducing reagents, we calibrated the concentrations of H_2O_2 and etoposide, and identified 100 and 10 μM, respectively, as concentrations that induced death at a similar rate to the death induced by the antibody and complement factors (Supporting Information Fig. S2C, S2D).

As determination of cell death by viability assays can be biased by cell cycle arrest or variations of the metabolic activity of mitochondria, we determined the actual death of tumor cells by an assay that relies on them releasing a fluorescently labeled dye (Cell tracker Orange). The cells were first labeled and then incubated for 24 h in the presence of the different cell death inducers (H_2O_2, etoposide and the antibody with complement factors), and the percentage cytotoxicity as measured by the release of the fluorescent dye to medium was calculated (Fig. 1A). We show that all death inducers, including the antibody and complement factors, significantly killed the tumor cells relative to the untreated cells and at similar rates. To make sure that the complement was activated in the presence of the antibody, we measured the concentrations of C3a, the product of the C3 proteolytic cleavage. Naturally, C3a was absence in the in vitro system in the absence of complement, and high levels were found when complement was added without the antibody, probably because the complement preparation was derived from mice serum (Fig. 1B). However, when both complement and antibody were preset, the levels of C3a were increased by 1.5-fold ($P < 0.001$) indicating complement activation.

3.3 | The 161-pAb and complement factors kill tumor cells by regulated necrosis

To determine the type of death that is induced by the 161-pAb antibody and complement, we next measured known markers of necrosis and apoptosis (Fig. 1B). H_2O_2 can kill cells by necrosis,[27] and thus we measured the activity of the enzyme LDH, which is often used to determine membrane permeability and cell rupture typical of necrosis.[28,29] Both cell types released LDH to the medium upon incubation with the antibody and complement (over 4.5-fold, $P < 0.05$, relative to untreated cells), as well as with H_2O_2, that served as positive control. In contrast, release of LDH to the medium was only marginal in the cells incubated with etoposide (known to induce apoptosis[30]) or in the untreated cells.

One of the hallmarks of apoptotic death is the fragmentation of nuclear chromatin and production of 3'-OH ends in the broken DNA strands.[29] This was used to determine whether the different reagents induced apoptotic death in the tumor cells, using both ELISA (Fig. 1B) and the TUNEL assay (Fig. 1C). Both cell types exhibited similarly elevated DNA fragmentation levels in cells treated with etoposide (known to induce apoptosis[30,31]) and with 161-pAb and complement factors (3–4-fold, $P < 0.001$, relative to untreated cells), whereas untreated cells or cells treated with H_2O_2 revealed low levels of DNA
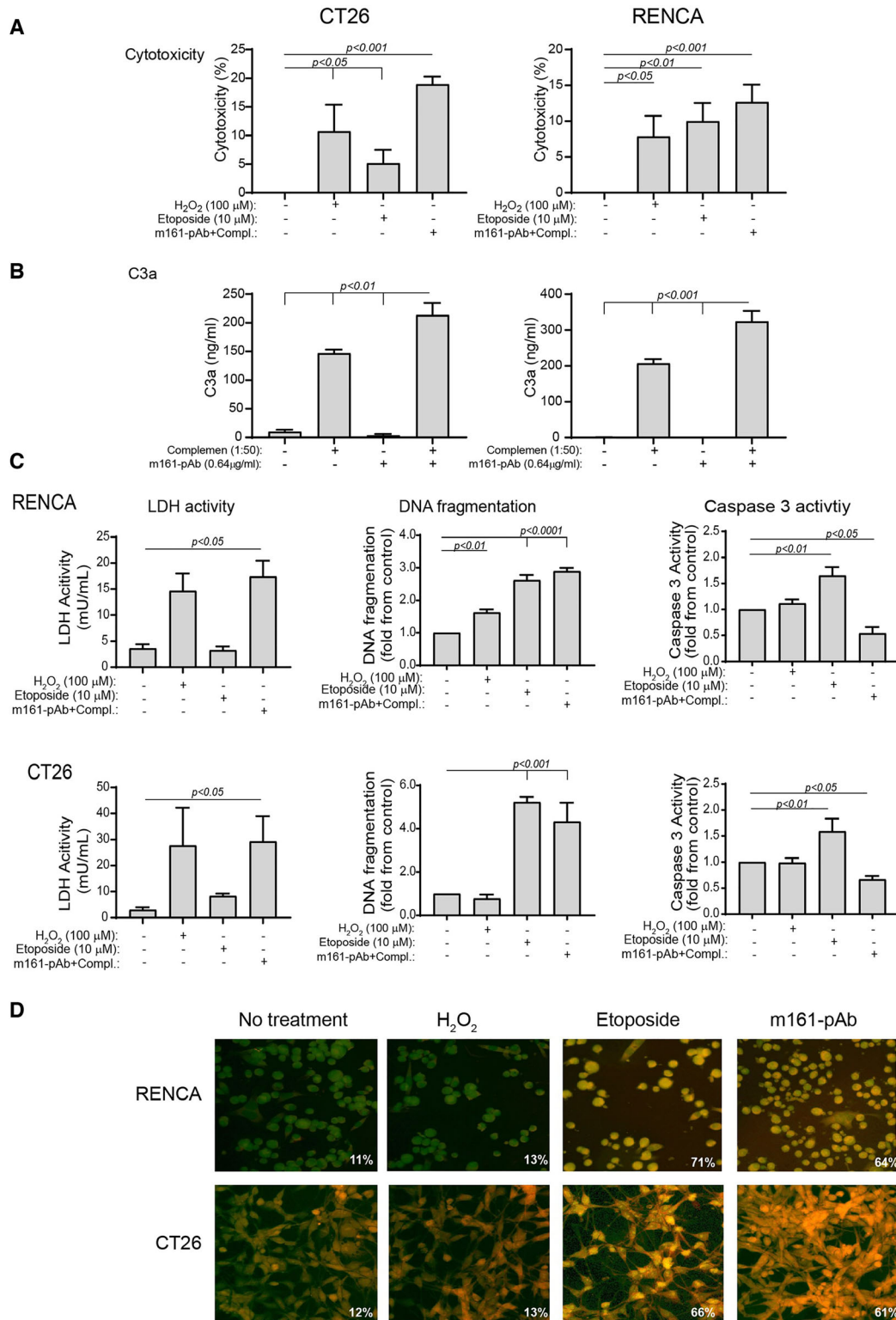
FIGURE 1 **Characteristics of the tumor cell death induced by 161-pAb and complement factors**. RENCA and CT26 cells were incubated in serum starvation medium for 24 h with H_2O_2 (100 μM), etoposide (10 μM) or the 161-pAb (0.64 μg/ml) and complement (diluted 1:50). (**A**) Tumor cells (2×10^4 cells) were labelled with Cell Tracker Orange prior to their incubation with the death inducers, and fluorescence in the supernatants indicated cell cytotoxicity calculated as described in Section 2 ("Methods") ($n = 5$ for CT26 cells, $n = 7$ for RENCA cells). (**B**) Tumor cells (2×10^5) were incubated with complement (diluted 1:50) and 161-pAb (0.64 μg/ml) and complement activation was assessed by the accumulation of C3a. (**C**) Cells (4×10^5 cells/well) were incubated with the death inducers, and LDH activity, a measure of necrosis, was measured in the conditioned media ($n = 4$–5). Fragmentation of DNA, and caspase-3 activity, both indicators of apoptosis, were measured in tumor cell lysates ($n = 5$-6). (**D**) Tumor cells were stained for DNA breaks (TUNEL assay, anti-BrdU in DNA breaks stained red, 7-aminoactinomycin D staining the DNA in cells in green). Percentage of double-positive staining are indicated (magnification ×250)

fragmentation. When we evaluated the activity of caspase-3, another marker of apoptotic death,[32] using its ability to cleave its specific substrate, we found that cells incubated with etoposide exhibited increased caspase-3 activity relative to the untreated cells (by 1.5–1.6-fold, $P < 0.01$), whereas cells subjected to H_2O_2 did not demonstrate a change in caspase-3 activity (Fig. 1B). Surprisingly, cells that were induced to die by 161-pAb and complement factors showed reduced caspase-3 activity relative to untreated cells (by 1.5–1.8-fold, $P < 0.05$).

Caspase-8 activity is a known checkpoint that dictates the choice of a specific death pathway. Increased activity of caspase-8 leads to death by apoptosis, whereas inhibited activity of caspase-8 may lead to the assembly of the necrosome complex.[7] We therefore, evaluated the activity of caspase-8, and found that similar to caspase-3, etoposide enhanced this activity (by 1.3-fold, $P < 0.05$) relative to the untreated cells or cells subjected to H_2O_2, and the 161-pAb and complement factors reduced it (by 1.4–1.5-fold, $P < 0.05$), pointing to necroptosis (Fig. 2A). Thus, 161-pAb and complement killed cells in a caspase-independent manner, ruling out apoptosis, despite the elevated DNA fragmentation.

Furthermore, incubating both tumor cells with necrostatin-1, an inhibitor of RIPK1 that is a key component of the necrosome, inhibited the 161-pAb-induced cell death (Fig. 2A). To ascertain that the necrosome components were indeed activated by 161-pAb, we evaluated the phosphorylation and expression of both RIPK3 and MLKL. We show that whereas the phosphorylation of RIPK3 was relatively minor in the untreated, H_2O_2- and etoposide-treated cells, and it was markedly increased by the 161-pAb and complement (by over 30-fold, $P < 0.01$). In comparison, both phosphorylation and expression of the MLKL protein were induced by this treatment relative to the untreated cells or other death-inducing treatments, resulting only in and moderate increased in the ratio between the phosphorylated and total protein (2.5-fold, $P < 0.05$) (Fig. 2B). Finally, we observed the phosphorylated forms of RIPK3 and MLKL at the plasma membrane of the tumor cells that were subjected to the antibody and complement, consistent with the known migration of the activated necrosome to the plasma membrane (Fig. 2C).

3.4 | Double-stranded RNA (dsRNA) released by the tumor cells activate an antiviral program in macrophages

During regulated necrosis, cells release DAMPs that might influence the TME. We assessed the release of three such DAMPs to the conditioned medium (CM). We demonstrate that killing of the tumor cells by the 161-pAb and complement factors did not change the release of ATP or IFNβ in comparison to untreated cells or cells induced to die by H_2O_2 or etoposide. In contrast, the release of dsRNA was markedly enhanced in the CM of tumor cells incubated with 161-pAb and complement factors relative to all other treatments (by about 3-fold $P < 0.01$, Fig. 3).

We next asked whether the release of DAMPs could change the activation mode of macrophages. First, we incubated the RAW 264.7 macrophage-like cells with the CM derived from tumor cells that were

incubated with the different death-inducers. After 24 h of incubation, we evaluated the secretion and accumulation of different cytokines. We show that macrophages incubated with CM from tumor cells treated with 161-pAb and complement factors moderately elevated their IL-1β and TNFα levels relative to macrophages incubated with CM from untreated cells (by 1.7- and 1.5-fold, respectively, $P < 0.05$, Fig. 4Aa–d). In contrast, TGFβ levels were not significantly changed (Fig. 4Af, Ah). Surprisingly, levels of IL-10, which is considered an anti-inflammatory cytokine, were markedly induced by the incubation with CM from cells that were induced to die with the 161-pAb and complement (by about 4-fold, $P < 0.001$, Fig. 4Ae, Ag). Although TNFα and IL-1β levels increased only moderately, IFNβ levels were markedly increased after incubation with CM derived from the tumor cells that were killed with the 161-pAb antibody and complement relative to all other treatments (by 3-fold for RENCA, $P < 0.05$ and by 4-fold for CT26 cell, $P < 0.01$, Fig. 4Ai, 4Ak). Moreover, RAW 264.7 macrophages that were incubated together with fresh tumor cells and CM from the 161-pAb and complement-induced dying tumor cells demonstrated increased cytotoxic abilities relative to the other treatments (by 7-fold for RENCA cells, $P < 0.001$ and by about 4-fold for CT26 cells, $P < 0.001$, Fig. 4Aj, Al). However, in the absence of macrophages, this CM was sufficient to kill only 10–15% of the fresh tumor cells compared to cells incubated with CM from untreated cells. Cumulatively, these results demonstrate that the dying cells can affect macrophages found in their vicinity in a paracrine manner.

We next asked whether the specific release of the dsRNA from tumor cells induced to die with the 161-pAb and complement factors (Fig. 3) has a role in the activation of the macrophages. To this end, we incubated RAW 264.7 macrophages with CM derived from untreated tumor cells, cells induced to die with 161-pAb and complement factors, or with the same CM that was first incubated with RNAse III that specifically digests dsRNA prior to its addition to the macrophages. We observed that secretion of IFNβ was increased when RAW 264.7 macrophages were incubated with the CM relative to the CM from untreated cells (by 3-fold for CT26, $P < 0.05$ and by 4-fold for RENCA cells, $P < 0.01$, Fig. 4Bm, Bp) as we have seen before (Fig. 4Ai, Ak). Moreover, the secretion of the cytokines IP-10/CXCL10 and TRAIL/TNFSF10 that are induced by the IFN response were also enhanced (by 3-fold for IP-10, $P < 0.01$, Fig. 4Bn, Bq and by 6-fold for TRAIL, $P < 0.05$, Fig. 4Bo, Br). However, when the CM was digested with RNAse III prior to its incubation with the macrophages, the elevation in the three cytokines was abolished (Fig. 4Bm–r).

3.5 | Mice vaccinated with 161-pAb demonstrate features of regulated necrotic cell death

To confirm that the mechanism described in the in vitro system occurs in vivo as well, we looked at a mouse RENCA tumor model that was treated with the 161-pAb anti-EMMPRIN antibody. We have previously described that the antibody changed the TME by increasing the local concentrations of IL-1β, TNFα, and nitrites while inhibiting TGFβ concentrations. Furthermore, macrophages infiltration into the tumor and their cytotoxic abilities were increased.[21] Because
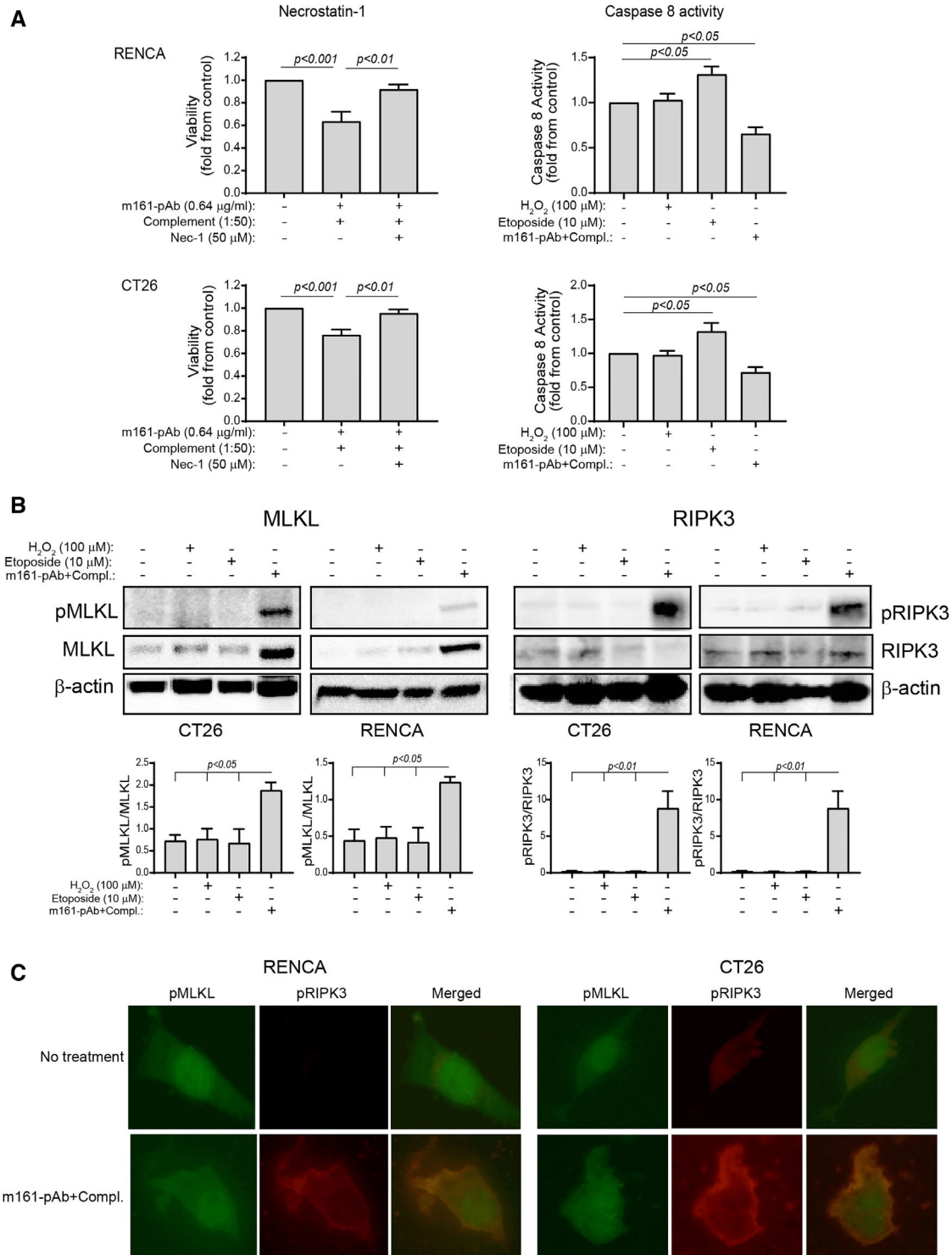
FIGURE 2   **The 161-pAb and complement factors kill tumor cells by regulated necrosis**. RENCA and CT26 cells were incubated in serum star-vation medium for 24 h with H_2O_2 (100 μM), etoposide (10 μM) or the 161-pAb (0.64 μg/ml) and complement (diluted 1:50). Some of the cells were pretreated with the receptor-interacting protein kinase 1 (RIPK1) inhibitor necroststain-1 (50 μM) for 1 h, as indicated. (**A**) Caspase-8 activity was measured in cell lysates ($n = 7$) and the ability of necroststain-1 to inhibit cell death measured by cell counting kit 8 (CCK-8; $n = 8$) suggested that 161-pAb and complement kill tumor cells by regulated necrosis (necroptosis-like). (**B**) Representative images of mixed-lineage kinase-like domain (MLKL) and RIPK3 phosphorylation and the ratio to the total expression of these proteins ($n = 4$ for each cell type) was enhanced only in the cells treated with 161-pAb and complement. (**C**) Representative images of untreated tumor cells or cells treated with 161-pAb and complement were stained with anti-phosphorylated-MLKL (green staining) and anti-phosphorylated-RIPK3 (red staining). The merged images show accumulation of both proteins at the plasma membrane only in treated cells (magnification ×800)
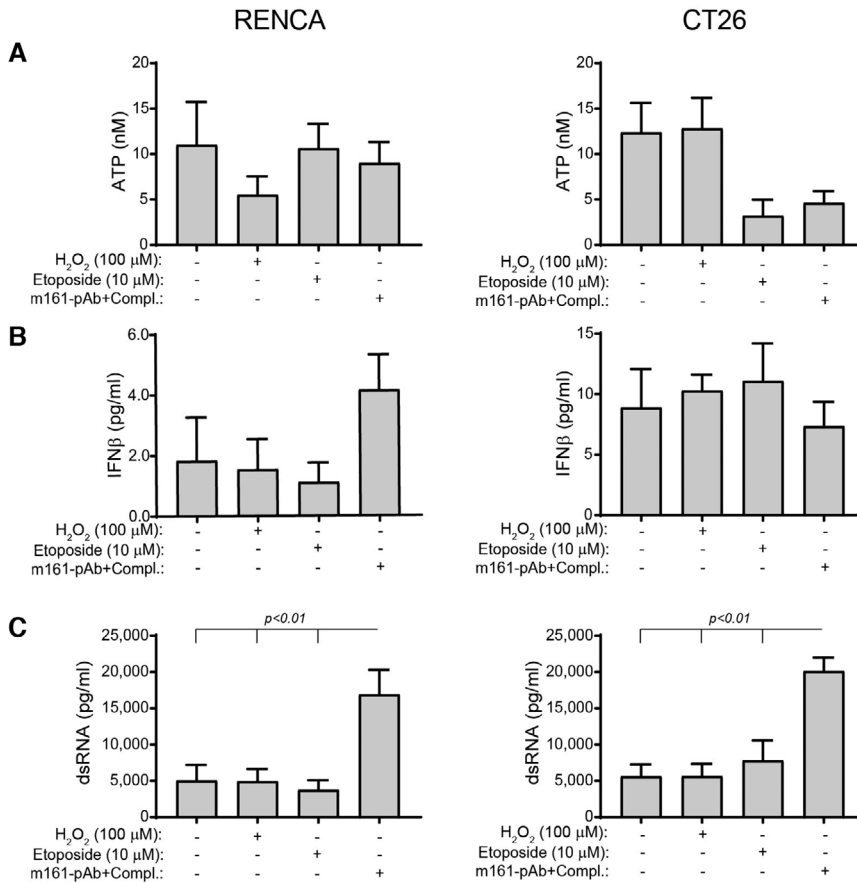
FIGURE 3 Cells treated with 161-pAb and complement release dsRNA. Selected danger-associated molecular patterns (DAMPs) released from CT26 and RENCA cells (4×10^5 cells) that were incubated in serum starvation medium for 24 h with H_2O_2 (100 μM), etoposide (10 μM), or the 161-pAb (0.64 μg/ml) and complement (diluted 1:50) were measured in the supernatants. (**A**) ATP ($n = 7$-8), (**B**) IFNβ ($n = 6$), and (**C**) dsRNA ($n = 6$)

CT26 and RENCA cells do not express iNOS,[26,33] it is most likely that the nitrites originated from M1-activated macrophages within the tumors. We now demonstrate that the markers of regulated necrosis are elevated in the tumor lysates extracted from tumor-bearing mice that were treated with 161-pAb relative to mice treated with a control antibody (rabbit-IgG). First, complement activation occurs in vivo in the presence of the 161-pAb antibody, as can be evaluated from the increased binding of the C3 cleaved product C3d to the tumor cells and necrotic tissue (Fig. 5A). The phosphorylated forms of RIPK3 and MLKL were increased in the 161-pAb treated tumors relative to control tumors (by 3- and 2-fold, respectively, $P < 0.05$, Fig. 5B,C). Likewise, the concentrations of dsRNA in lysates obtained from 161-pAb-treated mice were increased relative to the controls (by 1.7, $P < 0.0364$, Fig. 5D). The levels of IFNβ, IP-10, and TRAIL were also enhanced in the treated tumor lysates relative to the controls (by 77-, 22-, and 63-fold, respectively, $P < 0.05$, Fig. 5E–G). Moreover, macrophage activation within the tumors shifted from M2 activation to M1 activation, as demonstrated by the reduced gene expression of the M2-activation markers CD206 and Arg-I, and the increased gene expression of the M1-markers CD38 and iNOS (Fig. 5H–K). This change is not limited to macrophages only, as CD8$^+$ T cells demonstrate increased infiltration into the tumors, and can secrete more granzyme B, indicating their efficiency in the anti-tumor response (Fig. 5L–N).

4 | DISCUSSION

The main findings in our study are that the 161-pAb and complement factors cooperate to induce regulated necrosis in tumor cells leading to the selective release of dsRNA as DAMP, and to the subsequent activation of macrophages in a manner resembling an antiviral activation. To the best of our knowledge, this is the first time that an antigen-targeted therapy using an antibody and complement factors is shown to shift the mode of macrophage activation by triggering regulated necrotic death of the tumor cells.

First, our renewed analysis of our previously published RNAseq results[22] indicated that the 161-MAP vaccination triggered a broad-scope anti-tumoral response that resembles an antiviral response with a distinct ISG signature. This directed us to look for a mechanism that could explain how the IFN response was initiated and how it changed the TME. In two studies, we have previously demonstrated that vaccination with either an anti-EMMPRIN antibody (161-pAb) or a modified EMMPRIN peptide (161-MAP) resulted in a similar change of the TME. Because we have shown that 161-MAP vaccination triggered the production of anti-EMMPRIN polyclonal antibodies,[22] we concluded that the common denominator between these two approaches was the presence of anti-EMMPRIN antibodies. Therefore, we asked whether these antibodies were sufficient to trigger an IFN response that would change the TME.
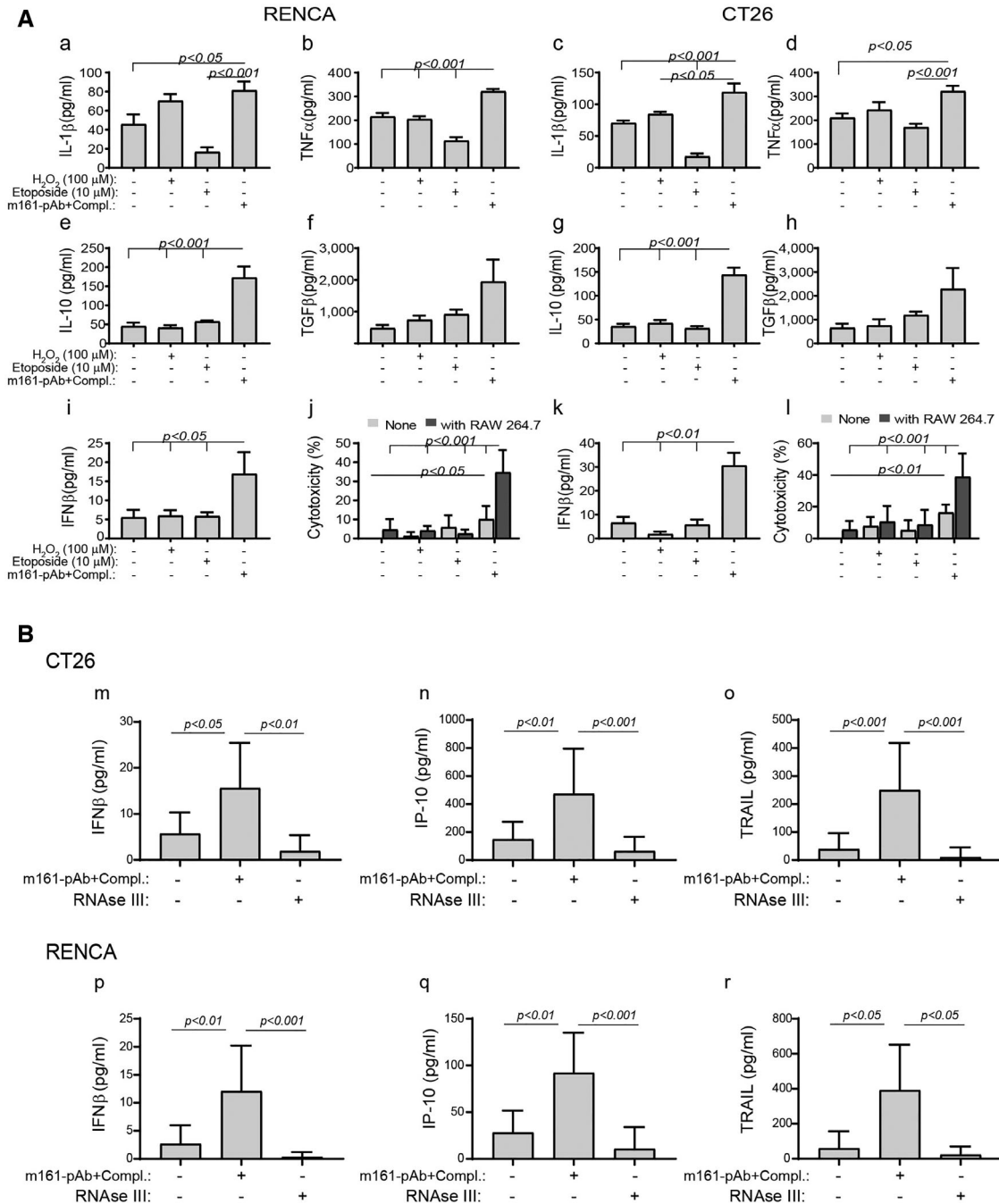
FIGURE 4 The dsRNA released by the tumor cells activates an antiviral program in macrophages. (**A a–i**, **k**) RENCA and CT26 cells were incubated with the death inducers as before, and the conditioned media were collected, and added to RAW 264.7 macrophages (5×10^5 cells) at a 1:1 ratio. After incubation of 24 h, supernatants were collected and cytokine concentration reflecting on macrophage activation were measured by ELISA ($n = 5$). (**Ai, Aj**) Fresh tumor cells (2×10^4 cells) were labeled with Cell Tracker, and then incubated with RAW 264.7 cells (10^4 cells) and the conditioned media from the tumor cells previously induced to die by the different cell inducers were added at a 1:1 ratio ($n = 6$). Florescence released from the cells indicated cell death that was calculated as described in the Section 2 ("Methods"). (**B**) Conditioned media from CT26 and RENCA cells (4×10^4 cells) that were untreated or incubated with the 161-pAb and complement factors as before, were added to RAW 264.7 macrophages (2×10^4 cells). Alternatively, the conditioned medium was first digested with RNAse III (10 U/ml for 30 min at 37°C) and then added to the macrophages at a 1:1 ratio. Concentrations of IFNβ, IP-10 and TRAIL were determined by ELISA ($n = 5$)

Using an in vitro system, we first showed that the combination of 161-pAb and complement was sufficient to trigger regulated necrotic death. We found that in cells induced to die by 161-pAb and complement, LDH activity and DNA fragmentation increased, whereas caspase-3 activity was inhibited. Increased LDH activity is strongly associated with increased cell permeability and rupture.[28] DNA fragmentation as a marker of DNA damage is found in different cell death pathways, including necroptosis.[34,35] Therefore, the
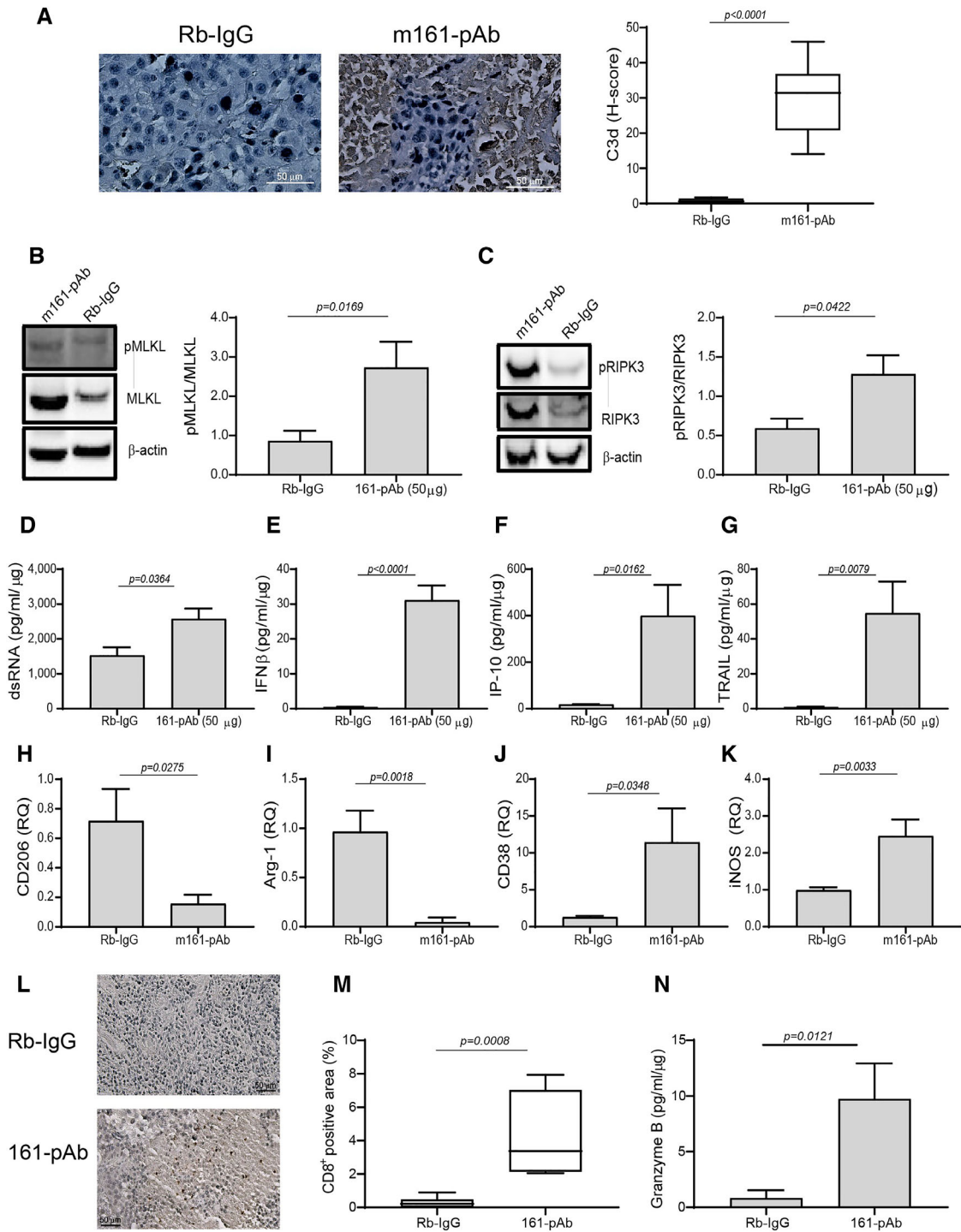
FIGURE 5 The 161-pAb treatment in RENCA tumor-bearing mice induced regulated necrosis. RENCA tumor cells (2×10^6 cells) were injected to the flank of BALB/c mice, and at day 12, when tumors became palpable, mice were i.p. injected with the 161-pAb (50 µg) every 7 d for a total of 3 boost injections. The negative control group received injections of an irrelevant antibody (rabbit-IgG). Mice were euthanized on day 39, and tumor lysates were extracted. Representative images of (**A**) C3d bound to tumor cells and its quantitation ($n = 4$), bar size is 50 µm. (**B**) phosphorylated and total mixed-lineage kinase-like domain (MLKL) and (**C**) phosphorylated and total receptor-interacting protein kinase 3 (RIPK3) and the quantitation of their ratio ($n = 4$). The concentrations of (**D**) dsRNA, (**E**) IFNβ, (**F**) IP-10, and (**G**) TRAIL were determined by ELISA ($n = 5$). The gene expression levels of the macrophages M2-activation markers (**H**) CD206 and (**I**) Arg-I, and the macrophages M1-activation markers (**J**) CD38 and (**K**) iNOS were assessed by qPCR ($n = 6$). (**L**) Representative images of CD8$^+$ T cell infiltration, (**M**) their quantification ($n = 5$), and (**N**) concentrations of granzyme B ($n = 6$)

finding that 161-pAb and complement increased both LDH activity and DNA fragmentation, but inactivated caspase-3, suggested a regulated, caspase-independent necrotic pathway. We therefore examined the typical molecules involved in necroptosis. Tumor cells that were incubated with 161-pAb and complement inhibited their caspase-8 activity, whereas cells incubated with the apoptosis-inducer etoposide increased it. Caspase-8 activity is an important checkpoint, and its inhibition is necessary for the triggering of necroptosis.[36] We could also show that both RIPK3 and MLKL were highly phosphorylated, suggesting that 161-pAb and complement activated them, and that MLKL expression was elevated after 24 h of treatment. This was in contrast to our controls of untreated cells, and cells induced to undergo necrosis by H_2O_2 or apoptosis by etoposide. Finally, we could show that preincubation with the RIPK1 inhibitor necrostatin-1 abolished the ability of the 161-pAb and complement to induce death. Cumulatively, these results suggest that the antibody and complement triggered a form of regulated necrosis, which is very similar to death-receptors-induced necroptosis.

These results are in agreement with a previous study that demonstrated the ability of the complement to activate RIPK1, RIPK3, and MLKL, and to induce a necroptosis-like cell death via complement-dependent cytotoxicity (CDC).[37] However, it is still unclear which signaling pathways activate these proteins. Likewise, the relative contribution of the complement factors and the antibody to this triggering are not yet described. It is likely that the antibody and the complement induce different pathways that collaborate to trigger the inactivation of caspase-8 and the activation of the necrosome. However, this merits further investigation. The inactivation of caspase-8 that allows the assembly of the necrosome is characteristic of necroptosis.[36,38,39] However, necroptosis usually requires triggering by the binding and activation of a death receptor, such as the receptors for TNFα, Fas, or TRAIL.[39] Our results show that both the complement and the anti-EMMPRIN antibody are required to induce regulated necrosis, without the activation of a specific death receptor. Because EMMPRIN is a receptor by itself, which binds to multiple proteins including itself via homophilic interactions,[40,41] we suggest that the binding of the antibody to the EMMPRIN receptor may activate a signaling pathway that later collaborates with the signaling triggered by the complement. However, this warrants a separate study and is beyond the scope of this paper. If proven correct, it may suggest that because not every antibody directed against any tumor-associated antigen will necessarily trigger such a regulated necrotic death, target selection in any potential therapy should take into account the ability of the target to trigger regulated necrosis.

We have previously demonstrated that vaccination resulted in increased infiltration of macrophages and CD8+ T cells into the tumor and enhanced their cytotoxicity.[21,22] Here we show that 161-pAb and complement are sufficient to induce regulated necrotic death that resembles necroptosis. Because necroptosis has been associated with induction of ICD,[42] and based on our previous results, we propose that the 161-pAb with complement can induce ICD in vivo. However, CDC that relies on the presence of both complement factors and the binding

of an antibody and drives necrotic death, has not been associated with ICD[43] until now.

Investigating how 161-pAb-induced cell death initiates ICD, we have shown that the death induced by 161-pAb and complement released high level of dsRNA to the CM, whereas the release of other DAMPs, such as ATP or IFNβ, did not change between the different treatments. This suggests that the type of cell death determines the nature, quantity, and immunogenicity of the DAMPs released.[7] Nucleic acids have been recognized as important DAMPs that activate immune cells, induce the IFN response,[44] and contribute to ICD.[6] Because the analysis of the RNAseq results indicated that the major dsRNA sensors, tlr3, Ddx58/RIG-I, and Ifih1/MDA5, were up-regulated, we predicted that dsRNA is involved. However, DNA sensors, such as Zbp1/DAI and Tmem173/STING were also elevated, suggesting that we have not yet identified all the relevant released DAMPs, or that the IFN response that followed the release of the dsRNA elevated these genes as part of the anti-tumoral program. We have verified that dsRNA was indeed specifically released by the regulated necrotic death, as necrosis or apoptosis did not release dsRNA above the basal level. However, the mechanism for the release of the dsRNA and its biochemical characterization were not investigated here, and it may originate from latent viral genomes, noncoding RNA, or tertiary structures of mRNA.

We next examined the effects of the 161-pAb-induced death on the shift of the immune suppressive TME into an immune permissive one. We chose to look at macrophages because of their prevalence in the TME, their ability to regulate the activity of other immune cells, and their central role in determining the immunosuppressive nature of the TME.[45] In the TME, macrophages are mostly activated as M2 macrophages that promote tumor progression, angiogenesis, and metastasis, and therefore, strategies to skew macrophages to their M1 mode of activation are of high importance.[46] We show that the regulated necrotic death shifted macrophage activity toward the antiviral M1 mode of activation. Although the secretion of proinflammatory cytokines (IL-1β, TNFα) was only moderately increased, we observed a marked elevation in secreted IFNβ. We note that the level of TFGβ, the main anti-inflammatory cytokine in the TME, was unchanged, and the marked elevation of anti-inflammatory IL-10 could be interpreted as an enhanced anti-tumoral response, due to its ability to stimulate cytotoxicity of CD8+ T cells.[47] The cytotoxic capabilities of the macrophages were enhanced after exposure to the CM obtained from cells treated with 161-pAb and complement, further indicating a shift toward M1 activation. These macrophages secreted not only IFNβ itself, but also other ISGs, such as IP-10/CXCL10 and TRAIL/TNFSF10, confirming our conclusion from the RNAseq results. Furthermore, the ability of macrophages to secrete IFNβ, IP-10, and TRAIL was abolished once the CM was digested with RNAse III, suggesting that the dsRNA was necessary to induce the IFN response in the macrophages.

Lastly, we showed that the regulated necrotic death also occurred in vivo, when we vaccinated tumor-bearing mice with the 161-pAb, as the phosphorylation of RIPK3 and MLKL, the levels of dsRNA, and the levels of IFNβ, IP-10, and TRAIL were all increased in the immunized mice relative to their controls. Furthermore, we demonstrated in vivo that

macrophage repolarization from M2- to an M1-activation mode does occur, and that CD8+ T cells enhance their infiltration into the tumor. Because tumor tissues were harvested at the end of the experiment after three boost injections of the antibody, and we did not observe in vivo the initial stages of macrophage polarization, we cannot categorically claim that macrophages are responsible for driving the gradual change in the TME. However, the central role of macrophages has been demonstrated by the in vitro system. Moreover, the importance of macrophages in determining the immunosuppressive TME and promoting tumor progression, as well as the anti-tumoral responses that their depletion evokes,[48–50] support our conclusion that macrophage repolarization drives the process of shifting the TME to allow an anti-tumoral response.

We conclude that 161-pAb together with complement factors is sufficient to initiate tumor cell death by regulated necrosis. This type of death is responsible for the secretion of dsRNA molecules, which are then taken up by the neighboring macrophages. The dsRNA is sufficient to skew macrophage activation toward the M1 activation, allowing the secretion of higher amounts of IFNβ, IP-10 and TRAIL. Over time and with repeated boost injections, this response may amplify itself, as more IFNβ and TRAIL are secreted and may continue to trigger necroptosis in tumor cells,[18] and more leukocytes, especially effector CD8+ T cells, are recruited to the site by IP-10.[51] This model is similar to therapy using oncolytic viruses, that cause tumor cells to die by ICD, release nucleic acids, and induce an IFN response that gradually changes the TME.[52] It is also possible that regulatory cells in the TME (e.g., TAMs, T regulatory cells) that express the TRAIL receptors[53,54] are gradually depleted, thus allowing a better anti-tumoral response. Thus, treatment with the anti-EMMPRIN antibody can gradually change the TME and might even prove beneficial in preventing tumor resistance to therapy. This model awaits further investigation.

ACKNOWLEDGMENTS

AUTHORSHIP

N.H., M.L., and E.S. carried out the experiments; S.K. reviewed and edited the manuscript; and M.A.R. designed the study, analyzed the results, and wrote the manuscript. N.H. and M.L. contributed equally to this work.

DISCLOSURES

The authors declare no conflicts of interest.

ORCID

Michal A. Rahat https://orcid.org/0000-0002-1881-1173

REFERENCES

1. Hanahan D, Weinberg RA. Hallmarks of cancer: the next generation. *Cell*. 2011;144:646-674.
2. Shen M, Kang Y. Complex interplay between tumor microenvironment and cancer therapy. *Front Med*. 2018;12:426-439.
3. Bonaventura P, Shekarian T, Alcazer V, et al. Cold tumors: a therapeutic challenge for immunotherapy. *Front Immunol*. 2019;10:1-10.
4. Sun Y. Tumor microenvironment and cancer therapy resistance. *Cancer Lett*. 2016;380:205-215.
5. Mpekris F, Voutouri C, Baish JW, et al. Combining microenvironment normalization strategies to improve cancer immunotherapy. *Proc Natl Acad Sci*. 2020;117:201919764.
6. Galluzzi L, Buqué A, Kepp O, et al. Immunogenic cell death in cancer and infectious disease. *Nat Rev Immunol*. 2017;17:97-111.
7. Pasparakis M, Vandenabeele P. Necroptosis and its role in inflammation. *Nature*. 2015;517:311-320.
8. Bénéteau M, Zunino B, Jacquin MA, et al. Combination of glycolysis inhibition with chemotherapy results in an antitumor immune response. *Proc Natl Acad Sci U S A*. 2012;109:20071-20076.
9. Obeid M, Tesniere A, Panaretakis T, et al. Ecto-calreticulin in immunogenic chemotherapy. *Immunol Rev*. 2007;220:22-34.
10. Martins I, Michaud M, Sukkurwala AQ, et al. Premortem autophagy determines the immunogenicity of chemotherapy-induced cancer cell death. *Autophagy*. 2012;8:413-415.
11. Apetoh L, Ghiringhelli F, Tesniere A, et al. Toll-like receptor 4-dependent contribution of the immune system to anticancer chemotherapy and radiotherapy. *Nat Med*. 2007;13:1050-1059.
12. Sukkurwala AQ, Martins I, Wang Y, et al. Immunogenic calreticulin exposure occurs through a phylogenetically conserved stress pathway involving the chemokine CXCL8. *Cell Death Differ*. 2014;21:59-68.
13. Garg AD, Vandenberk L, Fang S, et al. Pathogen response-like recruitment and activation of neutrophils by sterile immunogenic dying cells drives neutrophil-mediated residual cell killing. *Cell Death Differ*. 2017;24:832-843.
14. Galluzzi L, Vitale I, Aaronson SA, et al. Molecular mechanisms of cell death: recommendations of the Nomenclature Committee on Cell Death 2018. *Cell Death Differ*. 2018;25:486-541.
15. Vacchelli E, Ma Y, Baracco EE, et al. Chemotherapy-induced antitumor immunity requires formyl peptide receptor 1. *Science (80-)*. 2015;350:972-978.
16. Sistigu A, Yamazaki T, Vacchelli E, et al. Cancer cell-autonomous contribution of type I interferon signaling to the efficacy of chemotherapy. *Nat Med*. 2014;20:1301-1309.
17. Wallach D, Kang TB, Dillon CP, et al. Programmed necrosis in inflammation: toward identification of the effector molecules. *Science (80-)*. 2016;352:aaf2154.
18. Meng M-B, Wang H-H, Cui Y-L, et al. Necroptosis in tumorigenesis, activation of anti-tumor immunity, and cancer therapy. *Oncotarget*. 2016;7:57391-57413.
19. Landras A, Moura CRDe, Jouenne F, et al. CD147 is a promising target of tumor progression and a prognostic biomarker. *Cancers (Basel)*. 2019;11:1803. (17 pages).
20. Grass GD, Toole BP. How, with whom and when: an overview of CD147-mediated regulatory networks influencing matrix metalloproteinase activity. *Biosci Rep*. 2016;36:Article e00283. (16 pages).
21. Walter M, Simanovich E, Brod V, et al. An epitope-specific novel anti-EMMPRIN polyclonal antibody inhibits tumor progression. *Oncoimmunology*. 2015;5:e1078056. (12 pages).
22. Simanovich E, Brod V, Rahat MM, et al. Inhibition of tumor growth and metastasis by EMMPRIN multiple antigenic peptide (MAP) vaccination is mediated by immune modulation. *Oncoimmunology*. 2017;6:e1261778. (13 pages).
23. Bokarewa M, Tarkowski A, Lind M, et al. Arthritogenic dsRNA is present in synovial fluid from rheumatoid arthritis patients with an erosive disease course. *Eur J Immunol*. 2008;38:3237-3244.

24. Schonborn J, Oberstraß J, Breyel E, et al. Monoclonal antibodies to double-stranded RNA as probes of RNA structure in crude nucleic acid extracts. *Nucleic Acids Res*. 1991;19:2993-3000.

25. Schindelin J, Arganda-Carreras I, Frise E, et al. Fiji: an open-source platform for biological-image analysis. *Nat Methods*. 2012;9:676-682.

26. Simanovich E, Brod V, Rahat MM, et al. Function of miR-146a-5p in tumor cells as a regulatory switch between cell death and angiogenesis: macrophage therapy revisited. *Front Immunol*. 2018;8:article 1931. 16 pages).

27. Ali MAM, Kandasamy AD, Fan X, et al. Hydrogen peroxide-induced necrotic cell death in cardiomyocytes is independent of matrix metalloproteinase-2. *Toxicol Vitr*. 2013;27:1686-1692.

28. Chan FK, Moriwaki K, Rosa MJDe. Detection of necrosis by release of lactate dehydrogenase activity. *Methods Mol Biol*. 2013;979:65-70.

29. Kabakov AE, Gabai VL. Cell death and survival assays. In: Calderwood S, Prince T, eds. *Chaperones. Methods in Molecular Biology*. New York, NY: Humana Press; 2018:107-127.

30. Sverchinsky DV, Nikotina AD, Komarova EY, et al. Etoposide-induced apoptosis in cancer cells can be reinforced by an uncoupled link between Hsp70 and Caspase-3. *Int J Mol Sci*. 2018;19:1-15.

31. Park B, Je YT, Chun KH. AKT is translocated to the mitochondria during etoposide-induced apoptosis of HeLa cells. *Mol Med Rep*. 2015;12:7577-7581.

32. McComb S, Chan PK, Guinot A, et al. Efficient apoptosis requires feedback amplification of upstream apoptotic signals by effector caspase-3 or -7. *Sci Adv*. 2019;5:eaau9433. (11 pages).

33. Perske C, Lahat N, Sheffy Levin S, et al. Loss of inducible nitric oxide synthase expression in the mouse renal cell carcinoma cell line RENCA is mediated by microRNA miR-146a. *Am J Pathol*. 2010;177: 2046-2054.

34. Cui H, Zhu Y, Jiang D. The RIP1–RIP3 complex mediates osteocyte necroptosis after ovariectomy in rats. *PLoS One*. 2016;11:1-13.

35. Li Z, K Fan E, Liu J, et al. Cold-inducible RNA-binding protein through TLR4 signaling induces mitochondrial DNA fragmentation and regulates macrophage cell death after trauma. *Cell Death Dis*. 2017;8:e2775-16.

36. Tummers B, Green DR. Caspase-8: regulating life and death. *Immunol Rev*. 2017;277:76-89.

37. Lusthaus M, Mazkereth N, Donin N, et al. Receptor-interacting protein kinases 1 and 3, and mixed lineage kinase domain-like protein are activated by sublytic complement and participate in complement-dependent cytotoxicity. *Front Immunol*. 2018;9:Article 306. (14 pages).

38. Humphries F, Yang S, Wang B, et al. RIP kinases: key decision makers in cell death and innate immunity. *Cell Death Differ*. 2015;22:225-236.

39. Feoktistova M, Leverkus M. Programmed necrosis and necroptosis signalling. *FEBS J*. 2015;282:19-31.

40. Belton RJ, Chen L, Mesquita FS, et al. Basigin-2 is a cell surface receptor for soluble basigin ligand. *J Biol Chem*. 2008;283:17805-17814.

41. Knutti N, Kuepper M, Friedrich K. Soluble extracellular matrix metalloproteinase inducer (EMMPRIN, EMN) regulates cancer-related cellular functions by homotypic interactions with surface CD147. *FEBS J*. 2015;282:4187-4200.

42. Yang H, Ma Y, Chen G, et al. Contribution of RIP3 and MLKL to immunogenic cell death signaling in cancer chemotherapy. *Oncoimmunology*. 2016;5:1-13.

43. Galluzzi L, Buqué A, Kepp O, et al. Reply: the complement system is also important in immunogenic cell death. *Nat Rev Immunol*. 2017;17:143.

44. Wu J, Chen ZJ. Innate immune sensing and signaling of cytosolic nucleic acids. *Annu Rev Immunol*. 2014;32:461-488.

45. Poh AR, Ernst M. Targeting macrophages in cancer: from bench to bedside. *Front Oncol*. 2018;8:1-16.

46. Beltraminelli T, De Palma M. Biology and therapeutic targeting of tumour-associated macrophages. *J Pathol*. 2020;250:573-592.

47. Oft M. IL-10: master switch from tumor-promoting inflammation to antitumor immunity. *Cancer Immunol Res*. 2014;2:194-199.

48. Lopez-Yrigoyen M, Cassetta L, Pollard JW. Macrophage targeting in cancer. *Ann N Y Acad Sci*. 2020:1-24.

49. Malfitano AM, Pisanti S, Napolitano F, et al. Tumor-associated macrophages in cancer treatment. *Cancers (Basel)*. 2020;12: 1987-2012.

50. Long KB, Collier AI, Beatty GL. Macrophages: key orchestrators of a tumor microenvironment defined by therapeutic resistance. *Mol Immunol*. 2019;110:3-12.

51. Guo J, Xiao Y, Iyer R, et al. Empowering therapeutic antibodies with IFN-α for cancer immunotherapy. *PLoS One*. 2019;14:1-13.

52. Achard C, Surendran A, Wedge ME, et al. Lighting a fire in the tumor microenvironment using oncolytic immunotherapy. *EBioMedicine*. 2018;31:17-24.

53. De Looff M, De Jong S, Kruyt FAE. Multiple interactions between cancer cells and the tumor microenvironment modulate TRAIL signaling: implications for TRAIL receptor targeted therapy. *Front Immunol*. 2019;10:1-15.

54. Von Karstedt S, Montinaro A, Walczak H. Exploring the TRAILs less travelled: tRAIL in cancer biology and therapy. *Nat Rev Cancer*. 2017;17:352-366.

SUPPORTING INFORMATION

Additional information may be found online in the Supporting Information section at the end of the article.